L. I. Rudsinski, Phys. Rev. Lett. 28, 795 (1972); D. W. Forslund, J. M. Kindel, Kenneth Lee, E. L. Lindman, and R. L. Morse, Phys. Rev. A 11, 679 (1975).

[3]B. Ripin *et al.*, Phys. Rev. Lett. 34, 1313 (1975); E. Fabre and C. Stenz, Phys. Rev. Lett. 32, 823 (1974); C. Yamanaka, T. Yamanaka, T. Sasaki, and J. Mizui, Phys. Rev. Lett. 32, 1038 (1974); B. Ripin, Appl. Phys. Lett. 30, 134 (1977).

[4]K. R. Manes, H. G. Ahlstrom, R. A. Haas, and J. F. Holzrichter, Lawrence Livermore Laboratory Report No. UCRL-78771 (to be published).

[5]J. S. Pearlman, J. J. Thomson, and C. E. Max, Phys. Rev. Lett. 38, 1397 (1977).-

[6]P. Kolodner and E. Yablonovitch, Phys. Rev. Lett. 37, 1754 (1976).

[7]W. Mead *et al.*, Phys. Rev. Lett. 37, 489 (1976).

[8]W. Kruer, R. Haas, W. Mead, D. Phillion, and V. Rupert, in *Plasma Physics: Nonlinear Theory and Experiments*, edited by H. Wilhelmsson (Plenum, New York, 1977), pp. 64–81.

[9]R. A. Haas *et al.*, Phys. Fluids 20, 322 (1977).

[10]D. W. Phillion *et al.*, Lawrence Livermore Laboratory Report No. UCRL-78444 (to be published).

[11]E. K. Storm *et al.*, Lawrence Livermore Laboratory Report No. UCRL-79030 (to be published).

[12]D. R. Speck and F. Rienecker, Lawrence Livermore Laboratory Report No. UCRL 50021-74, 1974 (unpublished), p. 35.

[13]J. A. Glaze, Opt. Eng. 15, 136 (1976).

[14]S. R. Gunn, unpublished; S. R. Gunn and V. C. Rupert, to be published.

[15]V. L. Ginsburg, *The Propagation of Electro-magnetic Waves in Plasmas* (Pergamon, New York, 1969).

[16]V. W. Slivinsky, H. N. Kornblum, and H. D. Shay, J. Appl. Phys. 46, 1973 (1975).

[17]K. G. Estabrook and E. J. Valeo, Lawrence Livermore Laboratory Report No. UCRL 77146, 1975 (unpublished); J. J. Thomson and C. Randall, private communication.

[18]R. J. Faehl and W. L. Kruer, Phys. Fluids 20, 55 (1977); W. Manheimer, Phys. Fluids 20, 265 (1977).

[19]W. L. Kruer and K. G. Estabrook, in *Laser Interaction and Related Plasma Phenomena*, edited by H. Schwarz and H. Hora (Plenum, New York, to be published), Vol. 4.

[20]A. B. Langdon and B. F. Lasinski, in *Methods in Computational Physics*, edited by J. Killeen *et al.* (Academic, New York, 1976), Vol. 16.

Theory of Hot-Electron Spectra at High Laser Intensity

D. W. Forslund, J. M. Kindel, and K. Lee

Theoretical Division, Los Alamos Scientific Laboratory, Los Alamos, New Mexico 87545

(Received 17 January 1977)

A simple model involving resonant absorption in a self-consistent sharp density gradient is found to be in quantitative agreement with the suprathermal-electron spectrum from recent laser-plasma–interaction experiments and to explain qualitatively the scaling of that suprathermal-electron spectrum with laser power and wavelength.

There has been considerable controversy in recent years on the source of the hot or suprathermal electrons and high-energy x rays observed in high-powered–laser–target experiments.[1-5] We propose in this Letter a simple model which quantitatively agrees with experimental data from a variety of laboratories. In particular, we present an explanation as to why the hot-electron temperature in laser-produced plasmas at high incident laser intensity scales weakly with both laser wavelength and laser intensity. We find that at high laser power the self-consistent steepening of the plasma density profile in which the laser penetrates to densities greatly exceeding the critical density results in resonant absorption being the dominant absorption mechanism. At the same time the electron-heating mechanism of resonant absorption allows the steepened profile to persist. In this quasiequilibrium state this model predicts that the characteristic hot-electron energy, T_H, is given approximately (in keV) by

$$T_H \sim 14(I\lambda^2)^{1/3}T_c^{1/3}, \quad (1)$$

where I is the laser intensity in units of 10^{16} W/cm^2, λ is the laser wavelength in micrometers, and T_c is the background electron temperature in keV at the critical density.

At one point hot-electron temperatures were thought to scale as $I\lambda^2$ on the basis of infinite-homogeneous-plasma simulations or heat-capacity arguments.[6] Flux-limit arguments in which the bulk of the electrons are stochastically heated in a region around the critical density predict[7] that the electron temperature scales as $(I\lambda^2)^{2/3}$. In addition, the argument that the energy is car-

ried away by a thermal distribution results in the electron oscillating velocity $v_0 = eE_0/m\omega$ being less than the electron thermal velocity, v_e, where ω is the laser frequency and E_0 is the laser free-space electric field.[7] Resonant absorption has been observed in simulations[8,9] to give an electron energy which scales approximately as $(I\lambda^2)^{1/2}$.

In the presence of a two-temperature electron distribution, the above scaling laws and behavior of the density profile in the vicinity of the critical density are completely changed. For the case of resonant absorption at sufficiently high power where all the absorbed laser energy is carried away by a free-streaming, low-density high-energy electron component, we have

$$\alpha I = \beta n_H m v_H^3/2, \tag{2}$$

where α is the fraction of the incident flux absorbed: v_H is the hot-electron thermal velocity, $(T_H/m)^{1/2}$; n_H is the hot-electron density; and β is a number of order unity characterizing the energy carried by an almost Maxwellian distribution, and is 0.798 for a one-dimensional Maxwellian distribution. If the energy $T_H = mv_H^2/2$ of the hot electrons is determined by the acceleration process as it is in the case of resonant absorption, Eq. (2) will determine the number of hot electrons n_H. From Eq. (2) we can also see immediately that

$$\frac{v_0^2}{v_e^2} = \frac{E_0^2}{8\pi n_c T_c} = \frac{\beta v_H}{\alpha c}\frac{n_H T_H}{n_c T_c}, \tag{3}$$

where n_c is the critical density at which point the laser frequency matches the local plasma frequency, ω_p. If $n_H < n_c$, the hot electrons form a uniform background so that the local pressure gradients are due to the cold electrons even if $n_H T_H > n_c T_c$. Consequently, it is possible for v_0^2/v_e^2 to be much larger than unity. It is this inequality, $v_0^2/v_e^2 \gg 1$, that we define to mean high laser intensity. If we assume that the background temperature at solid density as determined from x-ray measurements is nearly the same as that at critical density (which will be more nearly true for sharp density gradients), we have that T_c is approximately 500 eV, nearly independent of laser power and wavelength. For this temperature the laser pressure tends to dominate the plasma pressure ($v_0/v_e > 1$) at 10^{13} W/cm^2 for 10-μm lasers and at 10^{15} W/cm^2 for 1-μm lasers.

At these high laser powers the laser penetrates the plasma until the plasma pressure balances the laser pressure:

$$n = E_0^2/8\pi T_c. \tag{4}$$

Note that, provided $n > n_c$, Eq. (4) indicates that a high-power laser will penetrate to a specified density independent of wavelength. For example, at 10^{15} W/cm^2 and $T_c = 300$ eV, the penetration density is of order 2×10^{21} cm^{-3}. Thus a 10-μm-wavelength CO_2 laser at this intensity will penetrate to a density about 200 times its critical density and, in fact, this transition from underdense to 200 times critical density occurs in a distance considerably less than a wavelength of light. This sharp density gradient results in resonant absorption being the dominant absorption mechanism. Furthermore, the fact that resonant absorption preferentially accelerates a small number of electrons in the tail of the distribution allows the steep density gradient to be maintained by pressure balance against the cold electrons. Basically, energy balance is satisfied by the hot electrons and momentum balance by the cold electrons.

In this new regime where the laser pressure balances the plasma pressure, it is important to determine the amount of absorption and the electron spectrum arising from the absorption and how these depend on intensity and wavelength. Although a scaling of T_H with $(I\lambda^2)^\delta$ for $\delta < \frac{1}{2}$ has been argued to be reasonable,[9] previous simulations have not observed this.[8,9] In order to determine the relevant physical processes, we have carried out a number of self-consistent particle-in-cell simulations with the two-dimensional, relativistic simulation code WAVE. What distinguishes these calculations from these earlier ones[8,9] is that for a given initial plasma temperature, we have chosen the plasma density profile so that there is approximate pressure balance. This allows for a more rapid determination of the equilibrium electron spectrum. Previous calculations have suffered from the plasma and laser light being out of equilibrium during most of the simulation. We find that the hot-electron energy is sensitive to deviations from this equilibrium. In these calculations we have varied the oscillating velocity v_0 by a factor of 4. Since $v_0 \propto (I\lambda^2)^{1/2}$, in the collisionless limit this is equivalent to varying $I^{1/2}$ or λ by a factor of 4. For a laser intensity of 10^{16} W/cm^2 with polarization in the plane of incidence, the wave vector of the laser at 20° to the density, and a background electron temperature of 2.5 keV, we have carried out simulations at five wavelengths, $\lambda = 0.7$, 1, 1.5,

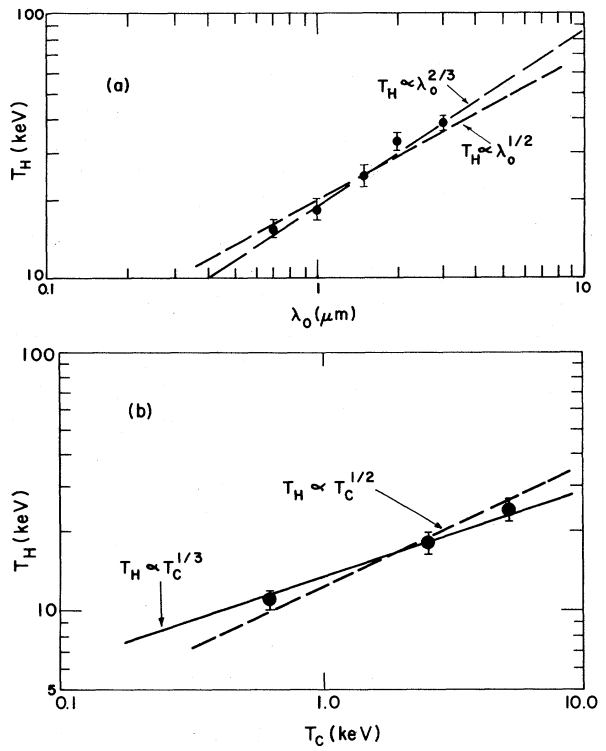

FIG. 1. (a) Measured hot-electron temperature as a function of laser wavelength for simulations with intensity equal to 10^{16} W/cm^2, background electron temperature $T_c = 2.5$ keV, the incident light wave incident at 20° to the density gradient and polarized in the plane of incidence, and ion- to electron-mass ratio of 100. Typically 250 000 simulation particles were used and $\Delta x \sim v_e/\omega_{p0}$. The error bars correspond to the variation of T_H with time. (b) Measured hot-electron temperature as a function of background temperature for simulations with the parameters of (a) except $\lambda = 1$ μm.

2, and 3 μm, corresponding to $v_0/c = 0.07$, 0.1, 0.15, 0.2, and 0.3. In each case the upper equilibrium density is 2.5×10^{21} cm^{-3} corresponding to 1.25, 2.5, 5.6, 10, and 23 times the respective critical densities. These simulations span the present experimental range of $I\lambda^2$ from 5×10^{15} to 10^{17} W μm^2/cm^2.

The results of these simulations are summarized in Fig. 1(a). In each case the absorption coefficient is found to be about 30%. There is no evidence of parametric instability; the absorption is essentially due to resonant absorption. The self-consistent profile adjusts itself until the density jumps from underdense to highly overdense in less than 10 Debye lengths at the critical density. The locally generated plasma wave in the steep density gradient is observed to deposit the absorbed laser energy in a high-energy tail to the electron distribution. This energy is convected to the boundary and absorbed with almost no heating of the background which would occur over the much larger electron mean free path. In Fig. 1(a) we plot the observed hot-electron energy as a function of wavelength (or equivalently as the square root of laser intensity). The mean hot-electron energy, T_H, is determined by fitting the observed hot-electron flux versus energy with the flux arising from a Maxwellian distribution. The fit is usually quite good[10] up to 5 times T_H. We see from Fig. 1(a) that a least-squares fit gives T_H scaling approximately as $(I\lambda^2)^{1/3}$ with an uncertainty of about ± 0.03 in the exponent.

We have also varied the background electron temperature (which also means varying the equilibrium density) at the intensity of 10^{16} W/cm^2 and $\lambda = 1$ μm. The results are shown in Fig. 1(b). Although we have a limited number of points, a least-squares fit yields T_H varying as $T_c^{1/3}$. Combining these fits to the data of Figs. 1(a) and 1(b) we obtain the result in Eq. (1).

In the simulations described above we find from direct measurement that $T_H \sim eEL$, where E is the magnitude of the local plasma-wave electric field and L is its scale length (cf., Ref. 7), defined to be the half-width of the plasma-wave density perturbation. This can be understood simply as the energy gained by a resonant electron falling through the localized wave potential $\Delta\varphi \sim EL$. At high laser intensities where the density gradient is very steep as just mentioned, the plasma-wave electric field is essentially equal to the incident laser electric field. This is true for a wide range of angles of incidence and is consistent with the 30% absorption mentioned above. The determination of T_H then reduces to the determination of the length L.

Although the rapidly varying electron density at the laser-plasma interface makes it difficult to define a scale length, there are five basic lengths which could characterize the local plasma-wave structure. For these nonrelativistic intensities, they are, in increasing order of size, v_e/ω_p, the upper-density Debye length; c/ω_{p0}, the upper-density electromagnetic skin depth; v_e/ω, the Debye length at the critical density; v_0/ω, the oscillating-electron excursion length in the incident field; and c/ω, the free-space incident light wavelength divided by 2π. Measurements of L in the simulations indicates that it is the geometric mean of c/ω_{p0}, v_e/ω, and c/ω.

By combining Eqs. (1) and (2), we find that in this high-power regime, the hot-electron density is given by

$$\frac{n_H}{n_c} = \alpha \frac{v_0}{v_c} = 2\alpha \frac{(I\lambda^2)^{1/2}}{T_c^{1/2}}, \quad (5)$$

where $I\lambda^2$ is in units of 10^{16} W $\mu m^2/cm^2$ and T_c is in keV. An approximate condition for this model to be valid (i.e., for the cold-electron temperature to dominate in pressure balance) is simply $n_H/n_c < 1$. Equation (5) implies $n_H < n_c$ only if $I\lambda^2 < 3\times10^{16}$ W $\mu m^2/cm^2$ for $\alpha = \frac{1}{3}$ and $T_c = 1$ keV. Since Eq. (5) assumes that the electrons make only one pass through the underdense plasma, the actual hot-electron density may be larger than this by the number of passes. The highest-power simulation of Fig. 1(a) has $n_H \sim n_c$ and still maintains the sharp density gradient. The fate of this equilibrium at significantly higher intensity is yet to be determined.

Experiments at Los Alamos Scientific Laboratory[2] for CO_2 and Nd-glass lasers at nearly the same intensity have indicated hot-electron temperatures which depend very weakly on laser wavelength. Giovanielli and McCall[2] have plotted the hot-electron temperature determined from x-ray and ion data from CO_2 and Nd lasers at various intensities from laboratories thoughout the world. A portion of this graph is shown in Fig. 2 as T_H versus $I\lambda^2$. The triangles represent 1.06-μm x-ray data, the open circles represent 10.6-μm x-ray data, and the squares represent 10.6-μm ion data. Note that the weak dependence of T_H on wavelength and intensity observed in the simulations appears to be reporduced in these data. The closed circles represent the hot-electron temperature from Fig. 1.

Since in the experiments the observed background temperature of about 500 eV is weakly dependent on laser power and wavelength, the region of strong profile steepening ($v_0/v_e \sim 1$) begins at about $I\lambda^2$ of 10^{15} W $\mu m^2/cm^2$. Below this power we expect that the hot-electron temperature is determined by other processes. Indeed, the dependence of the hot-electron energy on laser power and wavelength is different in this lower-power regime. The dependence may, in fact, be more in line with stochastic arguments as mentioned earlier. Using Eq. (2) to determine n_H for the low-power regime of Fig. 2 gives $n_H = 0.1 n_c$, so that either the heat flux is inhibited by a factor of 10 ($\beta = 0.1$) or only 10% of the electrons are stochastically heated. Which picture is valid can be determined by the fraction of the absorbed energy coming off in fast ions. Effects which alter the background temperature may also alter these scaling laws.

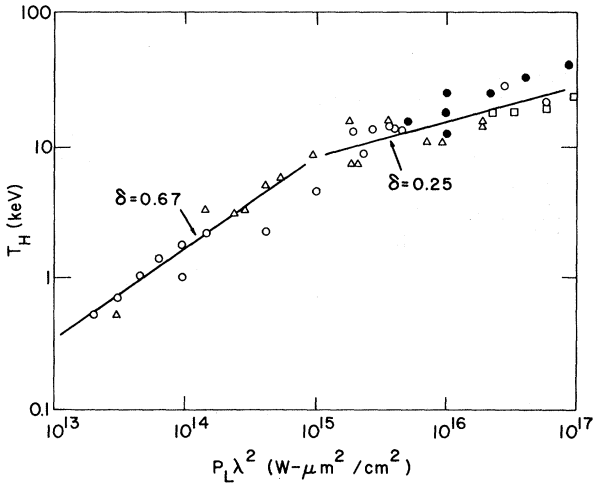

FIG. 2. Experimentally measured hot-electron temperature as a function of $I\lambda^2$. The measurements obtained from x rays are shown with triangles for 1.06-μm wavelength and open circles for 10.6-μm wavelength. The squares correspond to temperatures obtained from 10.6-μm ion data. The closed circles correspond to the simulations of Fig. 1. The solid curves are fits to the data of the form $T_H \propto (I\lambda^2)^\delta$. Note that $\delta = 0.67$ fits best for $I\lambda^2 < 10^{15}$ and $\delta = 0.25$ fits best for $I\lambda^2 > 10^{15}$.

This work was performed under the auspices of the U. S. Energy Research and Development Administration.

[1]Erik K. Storm, Bull. Am. Phys. Soc. 21, 1173 (1976); H. G. Ahlstrom, J. F. Holzrichter, R. A. Haas, E. K. Storm, K. R. Manes, D. W. Phillion, V. C. Rupert, M. J. Boyle, and K. M. Brooks, in Proceedings of the European Conference on Laser Interaction with Matter, Palaiseau, France, October 1976 (unpublished).

[2]D. V. Giovanielli and G. H. McCall, to be published, and references therein; D. V. Giovanielli, J. F. Kephart, and G. H. McCall, in *Proceedings of the IEEE International Conference on Plasma Science, Austin, Texas, 1976* (IEEE, New York, 1976), p. 97; Tai Ho Tan, D. V. Giovanielli, G. H. McCall, and A. H. Williams, *ibid.*, p. 95.

[3]B. H. Ripin, P. G. Burkhalter, F. C. Young, J. M. McMahon, D. G. Colombant, S. E. Bodner, R. R. Whitlock, D. J. Nagel, D. J. Johnson, N. K. Winsor, C. M. Dozier, R. D. Bleach, J. A. Stamper, and E. A. McLean, Naval Research Laboratory Report No. 3315, 1976 (unpublished), pp. 100–177.

[4]F. C. Young, R. R. Whitlock, R. Decoste, B. H. Ripin, D. J. Nagel, J. A. Stamper, J. M. McMahon, and S. E. Bodner, Appl. Phys. Lett. 30, 45 (1977).

[5]P. Kolodner and E. Yablonovitch, Phys. Rev. Lett.

37, 1754 (1976).
[6]G. I. Kachen, Jr., W. Clements, and M. Genin, Lawrence Livermore Laboratory Report No. UCRL-50021-72-1, 1972 (unpublished), pp. 110–111; W. L. Kruer and J. M. Dawson, Phys. Fluids 15, 446 (1972).
[7]R. L. Morse and C. W. Nielson, Phys. Fluids 16, 909 (1973); W. M. Manheimer, D. G. Colombant, and B. H. Ripin, Phys. Rev. Lett. 38, 1135 (1977).
[8]D. W. Forslund, J. M. Kindel, K. Lee, E. L. Lindman, and R. L. Morse, Phys. Rev. A 11, 679 (1975); K. G. Estabrook, E. J. Valeo, and W. L. Kruer, Phys. Fluids 18, 1151 (1975).
[9]E. Valeo, W. Kruer, K. Estabrook, B. Langdon, B. Lasinski, C. Max, and J. Thomson, in *Proceedings of the Sixth International Conference on Plasma Physics and Controlled Nuclear Fusion Research, Berchtesgaden, West Germany, 1976* (International Atomic Energy Agency, Vienna, 1976), paper No. IAEA-CN-35/F4; and B. Bezzerides, D. F. DuBois, D. W. Forslund, J. M. Kindel, K. Lee, and E. L. Lindman, *ibid.*, paper No. IAEA-CN-35/F3.
[10]K. G. Estabrook, private communication.

Electronic Structure of Catalytic Metal Clusters Studied by X-Ray Photoemission Spectroscopy

M. G. Mason, L. J. Gerenser, and S.-T. Lee
Research Laboratories, Eastman Kodak Company, Rochester, New York 14650
(Received 7 April 1977)

Pd and Pt clusters on carbon substrates have been studied by x-ray photoemission spectroscopy (XPS). Variations in valence- and core-level spectra with cluster size have been observed. Single-atom centers appear to exist in the d^9s^1 configuration. The d-electron count increases with cluster size, and in the case of Pt a correlation between d-orbital occupation and catalytic activity in electroless nickel deposition is observed.

We have chosen x-ray photoemission spectroscopy (XPS) to study the electronic structure of Pd and Pt nuclei supported on amorphous carbon substrates. The nuclei are prepared by vapor deposition onto the previously evaporated carbon films. Details of sample preparation and variation in cluster-size distribution with metal coverage have been previously reported.[1] The spectra were recorded on a Hewlett-Packard 5950A ESCA (electron spectroscopy for chemical analysis) spectrometer. Binding energies were referenced to the carbon 1s line of the substrate, which was assigned a value of 284.6 eV. This value was consistent with a zero binding energy for the Pd and Pt Fermi edges at high coverage. The valence-band (VB) spectra were corrected by subtraction of the carbon background and inelastic-scattering tail.[2] The corrected VB spectra of Pd and Pt nuclei are shown in Figs. 1 and 2. These spectra cover the range from isolated single atoms to bulklike clusters.[1] The evolution of the bulk spectra occurs in a continuous manner as the coverage is increased and is virtually complete above ~ 3×10^{15} atoms/cm^2. In addition to the VB spectra, we have also measured 3d (4d) core binding energies for Pd (Pt).

Spectra at the lowest coverages will be discussed first since these originate almost completely from single-atom centers.[1] The ground-state free-atom configurations for Pd and Pt are $4d^{10}$ and $5d^96s^1$, respectively.[3] However, in both

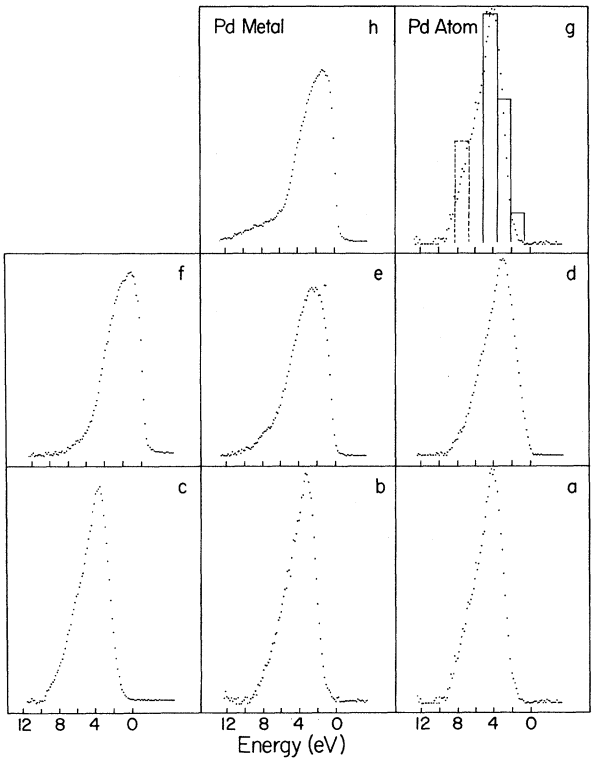

FIG. 1. The XPS spectra of Pd nuclei after background subtraction. The coverages in atoms cm^{-2} are (a) 2×10^{14}; (b) 4×10^{14}; (c) 8×10^{14}; (d) 1.6×10^{15}; (e) 3.1×10^{15}; (f) 6.2×10^{15}; (g) 2×10^{14}; and (h) bulk metal. The histogram in (g) represents the spectral profile for ionization of Pd in the d^9s^1 configuration. The calculated ^2S state is dashed (see text).